

## Parallel Connection and Sandwich Electrodes Lower the Internal Resistance in a Microbial Fuel Cell

Areli Ortega-Martínez<sup>1</sup>, Katy Juárez-López<sup>2</sup>, Omar Solorza-Feria<sup>3</sup>, María T. Ponce-Noyola<sup>4</sup>, Elvira Ríos-Leal<sup>5</sup>, Noemí F. Rinderknecht-Seijas<sup>6</sup> and Héctor M. Poggi-Varaldo<sup>1,\*</sup>

<sup>1</sup>Environmental Biotechnology and Renewable Energies R&D Group, Dept. Biotechnology & Bioengineering, Centro de Investigación y de Estudios Avanzados del I.P.N.

<sup>2</sup> Dept. Ingeniería Celular y Biocatálisis, Instituto de Biología, Universidad Nacional Autónoma de México, Cuernavaca, Mor. México

<sup>3</sup>Dept. of Chemistry, Centro de Investigación y de Estudios Avanzados del I.P.N. México

<sup>4</sup>Microbial Genetic Group., Dept. of Biotechnology & Bioengineering, Centro de Investigación y de Estudios Avanzados del I.P.N.

<sup>5</sup>Central Analítica, Dept. of Biotechnology & Bioengineering, Centro de Investigación y de Estudios Avanzados del I.P.N.

<sup>6</sup>Escuela Superior de Ingeniería Química e Industrias Extractivas – Instituto Politécnico Nacional, México D.F., México

Received: December 05, 2011, Accepted: February 01, 2012, Available online: April 02, 2012

**Abstract:** The aim of this work was to design and characterize a novel, multiface parallelepiped MFC in the perspective of decreasing the internal resistance ( $R_{int}$ ) and increasing the volumetric power ( $P_v$ ) output. The cell was fitted with a 'sandwich' cathode-membrane-anode assemblage in five of its faces, and possessed a ratio electrode surface area-to-volume  $\xi$  (csi) of  $19 \text{ m}^{-1}$ .

When the 5 faces of the MFC-P were connected in series, the  $R_{int}$  was  $601 \Omega$  with a voltage of  $0.52 \text{ V}$ . Characterization of the cell with the 5 faces connected in parallel gave a  $R_{int}$  of  $62 \Omega$  with a voltage of  $0.5 \text{ V}$  that corresponded to external resistance of  $56 \text{ k}\Omega$  in the polarization procedure. This result was ascribed to both the changes in cell architecture and decrease of the inter-electrode distance as well as the parallel connection. The  $P_v$  of the new MFC-P achieved values of  $62$  and  $570 \text{ mW/m}^3$  for series and parallel connection, respectively.

Molecular ecological techniques were used to analyze the bacterial diversity of biocatalyst used in new design MFC-P. They showed a low species richness and low-to-moderate evenness. The community consisted primarily of  $\delta$ -Proteobacteria and Firmicutes, bacteria that are recognized to be capable of exocellular electron transfer.

**Keywords:** internal resistance, microbial fuel cell, parallel. parallelepiped, series

### 1. INTRODUCTION

A microbial fuel cell (MFC) is a promising technology for generating electricity directly from biodegradable compounds using bacteria under anaerobic conditions [1,2]. In the anodic chamber the microorganisms anoxically oxidize the organic matter and release electrons and protons. Electrons are transported to the anode that acts as an intermediate, external electron acceptor. The electrons flow through an external circuit where there is a resistor or a device to be powered, producing electricity and finally react at

the cathode with the protons and oxygen producing water [1]. The corresponding protons released during the oxidation of organic compounds migrate to the cathode through the electrolyte (liquor) contained in the cell and a proton exchange membrane; in this way charge neutrality is kept [3,5].

The actual voltage output of an MFC is less than the predicted thermodynamic ideal voltage due to irreversible losses. The three major irreversibilities that affect MFC performance are: activation losses, ohmic losses, and mass transport losses. These losses are defined as the voltage required to compensate for the current lost due to electrochemical reactions, charge transport, and mass transfer processes that take place in both the anode and cathode com-

\*To whom correspondence should be addressed: Email: hectorpoggi2001@gmail.com  
Phone: 5255 57473800 x4324

**ABBREVIATIONS**

A	surface area of electrode (usually the anode)
CMA	'sandwich' arrangement cathode-membrane-anode
COD	chemical oxygen demand
$E_{MFC}$	MFC voltage
$I_{MFC}$	current intensity
L	length of separation between anode and cathode
MFC	microbial fuel cell
MFC-P	new design of microbial fuel cell in this work
MFC-S	standard microbial fuel cell in this work
$P_{An-max}$	maximum power density
$P_{MFC}$	MFC power
$P_{V-max}$	maximum volumetric power
PCR	Polymerase chain reaction
PEM	proton exchange membrane
$R_{ext}$	external resistance
$R_{int}$	internal resistance
$R_{ohmic}$	ohmic resistance
$R_{ion}$	Ionic resistance
$V_{MFC}$	MFC operation volume
VSS	volatile suspended solids

*Greek characters*

$\xi$	ratio surface-of-electrode to cell volume
$\kappa$	specific conductance or conductivity
$\rho$	specific resistance or resistivity

partments [5,6]. The extent of these losses varies from one system to another [7]. The electrochemical limitations on the performance of MFC are due to the internal resistance ( $R_{int}$ ). The primary component of  $R_{int}$  is ohmic resistance, which can be further divided into the electrolytic resistance and ohmic resistance of electrodes, and the transfer resistance electrodes.

The  $R_{ohmic}$  is typically dominated by the  $R_{ion}$  associated to the electrolyte(s) resistance [6,7]. The  $R_{ion}$  due to electrolyte is given by the following expression [8].

$$R_{ion} = \rho * L/A = (1/\kappa) * L/A \quad (1)$$

where  $\rho$ : specific resistance or resistivity of the electrolyte, L: distance between electrodes; A: electrode surface area;  $\kappa$ : specific conductance or conductivity of the electrolyte. Inspection of Eq. 1 draws our attention to the ways to lower ohmic losses, i.e., by reducing the distance that separates the electrodes (decreasing L), increasing the electrode surface area (increasing A), and increasing the conductivity of the electrolyte and materials of the proton-exchange membrane (increasing  $\kappa$ ). A plausible physical picture of the effect of inter-electrode separation would be that the protons have less distance to travel, and consequently the ohmic resistance is lowered.

The influence of electrode spacing on performance of MFCs has been shown in several works [5,9-13]. Another variable that may lead to lower  $R_{ohmic}$  is the electrode area. The latter can be expressed in terms of a variable  $\xi$ , the ratio of surface area of electrode to the cell volume, as follows:

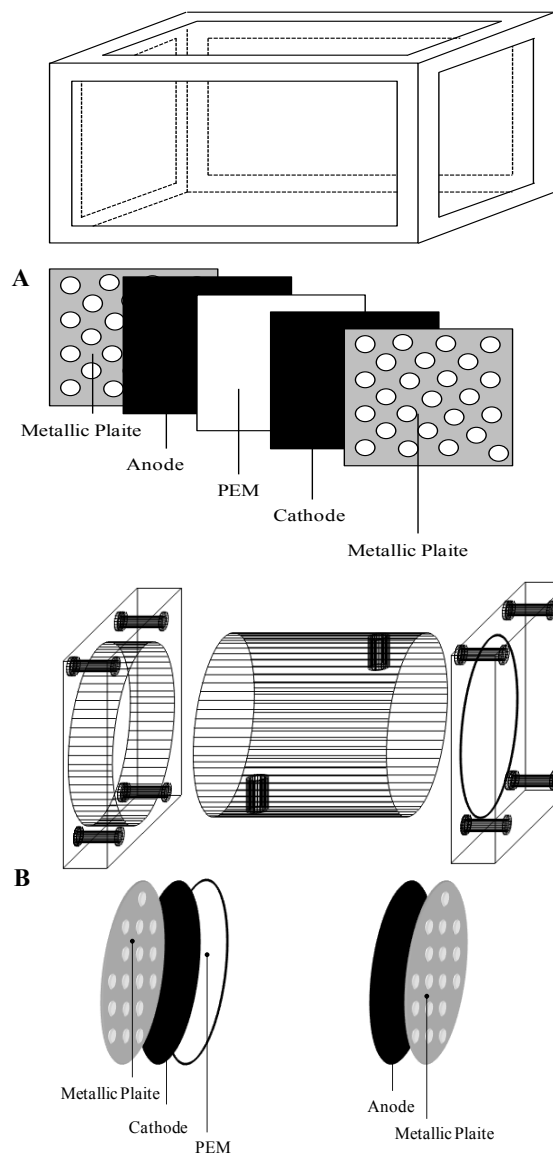


Figure 1. Schematic diagrams of microbial fuel cells: (A) type P (new design), and (B) type S (standard design).

$$\xi = A/V_{MFC} \quad (2)$$

where  $V_{MFC}$ : volume of the MFC. Several works have investigated the use of electrode materials with high  $\xi$ , such as granular and reticulated graphite and granular activated carbon [4,14]. Regarding the use of flat electrodes, the  $\xi$  of the cell can still be increased if more walls of the cell are fitted with electrodes.

The aims of this work were to design and characterize a novel, multiface parallelepiped MFC-P in the perspective of decreasing the  $R_{int}$  and increasing the volumetric power ( $P_v$ ) output, and analyse the microbial diversity in the biocatalyst used in new design MFC-P. The cell was fitted with a 'sandwich' cathode-membrane-anode assemblage, and possessed a high ratio electrode surface area-to-volume  $\xi$  (csi).

## 2. EXPERIMENTAL

### 2.1. Microbial fuel cell architecture

The new design MFC-P consisted of a parallelepiped built in plexiglass with a liquid volume of 0.977 L (Fig. 1A). Five faces of this cell were fitted with ‘sandwich’ cathode-membrane-anode assemblages (CMA). Each CMA (from inside to outside) consisted of an anode made of Toray carbon cloth, the proton exchange membrane (Nafion 117), and the cathode made of flexible carbon-cloth containing 0.5mg/cm<sup>2</sup> Pt catalyst (Pt 10 wt%/C-ETEK, and a perforated plate of stainless steel 1 mm thickness.

On the other hand, a standard cell (Fig. 1B) of 150 mL MFC-S was fitted with a circular anode made of stainless steel plate 1 mm thickness with a Toray flexible carbon-cloth sheet placed in one circular face and a cathode in the opposing face made of (from inside to outside): proton exchange membrane (Nafion 117), a Toray flexible carbon-cloth painted with Pt catalyst, and a perforated plate of stainless steel 1 mm thickness. Separation between electrodes was 7.8 cm.

The MFC-P had a ratio  $\xi = 19.1$  (1/m) whereas the corresponding value of the standard MFC-S was 12.9 (1/m).

### 2.2. Synthetic feed and Biocatalyst

The MFC-S and MFC-P, were loaded with 7 and 46 mL, respectively, of a synthetic feed [15-17]. The synthetic feed was consisted of a mixture of the following substances (in g/L): acetic, propionic and butyric acids (4 each) as well as acetone and ethanol (4 each) and mineral salts such as NaHCO<sub>3</sub> and Na<sub>2</sub>CO<sub>3</sub> (3 each) and K<sub>2</sub>HPO<sub>4</sub> and NH<sub>4</sub>Cl (0.6 each). Organic matter concentration of synthetic feed was ca. 25 g COD/L. The cells, MFC-S and MFC-P, were loaded with 143 and 954 mL, respectively, of mixed liquor from a sulphate-reducing, mesophilic, complete mixed, continuous bioreactor. The bioreactor had an operation volume of 3 L and was operated at 21 day hydraulic retention time and 35°C in a constant temperature room. The bioreactor was fed at a flow rate of 150 mL/d with an influent whose composition was (in g/L): sucrose (5.0), Acetic acid (1.5), NaHCO<sub>3</sub> (3.0), K<sub>2</sub>HPO<sub>4</sub> (0.6), Na<sub>2</sub>CO<sub>3</sub> (3.0), NH<sub>4</sub>Cl (0.6), plus sodium sulphate (7.0), the pH in the bioreactor liquor was 7.2. The initial COD and biomass concentration in cells liquor were ca. 1 450 mg O<sub>2</sub>/L and 1100 mg VSS/L. The initial and final pH and sulfide concentration in cells liquor were 7.66 and 7.8, and 9.7 and 16.7 mmol/L respectively. Electrical conductivity of cell liquor was 2020 mS/m.

### 2.3. Determination of internal resistance of the cells

The internal resistance of cells was determined using the polarization curve method and EIS.

#### 2.3.1. Polarization curve method

The polarization curve was carried out by varying the external resistance ( $R_{ext}$ ) and monitoring both the voltage and the current intensity, according to procedures suggested by Clauwaert *et al.* (2007) [18] and Logan *et al.* (2006) [1]. For the MFC-P, characterization was first carried out with the five faces connected in series and second with faces connected in parallel. In brief, each MFC was loaded with substrate and inocula as described in section 2.2. Each MFC was batch-operated for 8 h at room temperature. The circuit of the MFC was fitted with an external variable resistance. In this regard, we carried out the polarization curve of the MFC,

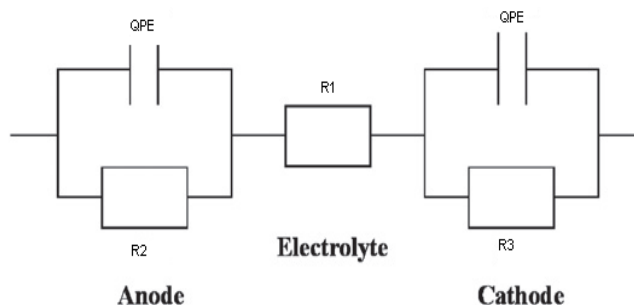


Figure 2. The schematic of a MFC and its equivalent circuit:  $R_1$  – solution resistance (ohmic resistance),  $R_2$  – anodic polarization resistance,  $R_3$  – cathodic polarization resistance and QPE – constant phase element.

relating mathematically the cell voltage ( $E_{MFC}$ ) and current intensity ( $I_{MFC}$ ) against the external resistance value, forwards and backwards regarding the  $R_{ext}$  values. *Ab initio*, the MFC was operated at open circuit for 1 h. Afterwards, the  $R_{ext}$  was varied from 100  $\Omega$  to 1 M $\Omega$  and viceversa. After this, the cell was set to open circuit conditions for 1 h in order to check the adequacy of the procedure (values of initial and final open circuit voltages should be close). The voltage was measured and recorded with a multimeter. The current was calculated by the Ohm’s Law as indicated below in Section 2.4.

### 2.3.2. Electrochemical Impedance Spectroscopy (EIS)

A Gamry PCI4/300 potentiostat was used for all electrochemical measurements. Gamry EIS300 software was used for recording of impedance spectra, while DC105 software was used for recording of potential sweeps, monitoring of the potential difference between the two reference electrodes and for measuring the I–t curve at an applied cell voltage.

For the MFC-P, characterization was first carried out with the five faces connected in series and second with faces connected in parallel. EIS measurements were carried out for the MFC in a frequency range of 1 MHz to 10 mHz with an ac signal of 10 mV amplitude, these measurements were performed for the MFC at several applied cell voltages, the anode was used as the working electrode and the cathode was used as the reference as well as the counter electrode. The results of impedance measurement were represented in a Nyquist plot. It expresses the impedance with a real part and an imaginary part as a semicircle. Each point on the complex plane plot represents the impedance at a certain frequency.

Accurate results are obtained by fitting the impedance data to an appropriate equivalent circuit. The equivalent circuit used in this work is shown in Fig. 2, which has elements:  $R_1$ - solution resistance (ohmic resistance),  $R_2$ - anodic polarization resistance,  $R_3$ - cathodic polarization resistance and QPE- constant phase element. The sum of  $R_1$ ,  $R_2$  y  $R_3$  will be  $R_{int}$ .

### 2.4. Analytical methods and calculations

The COD, VSS, pH, sulfide, electrical conductivity in liquors of sulphate-reducing seed bioreactor and cells were determined ac-

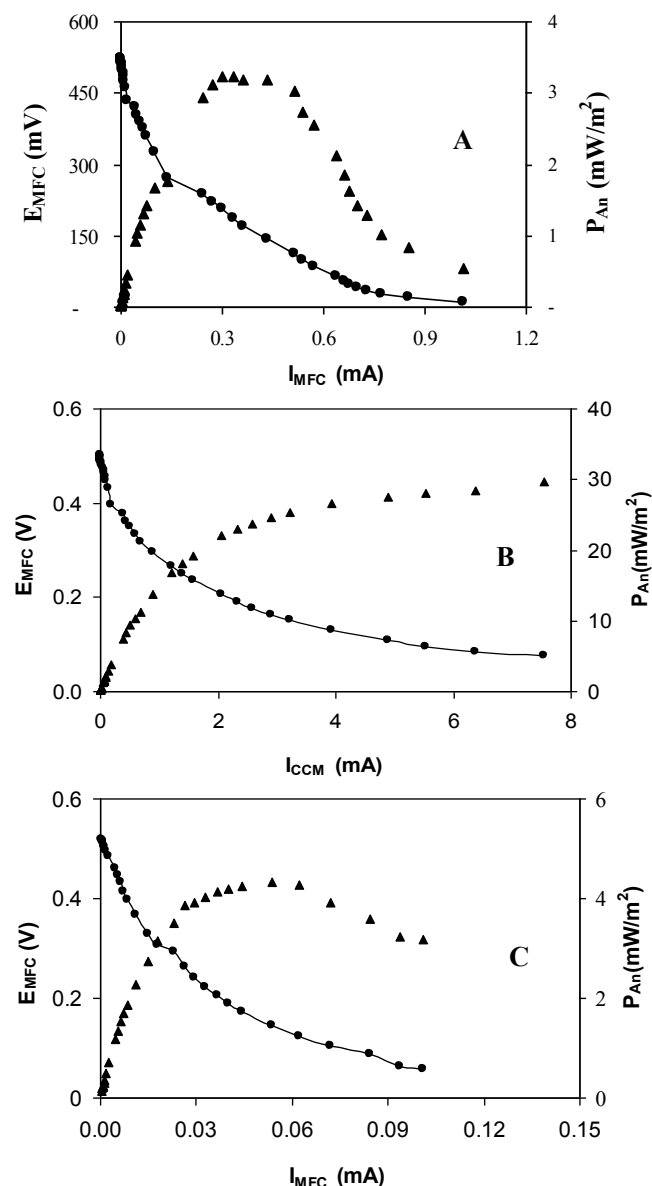


Figure 3. Polarization curves of new design microbial fuel: (A) connection in series and (B) connection in Parallel. (C) standard microbial fuel cell

according to the Standard Methods [19]. The current intensity  $I_{MFC}$ , the power  $P_{MFC}$  and the power density  $P_{An}$  were determined as reported elsewhere [16].

The power per unit volume or volumetric power  $P_V$  was calculated as follows:

$$P_V = \frac{E_{MFC}^2}{V_{MFC} \cdot R_{ext}} \quad (3)$$

where  $R_{ext}$  is the external resistance,  $E_{MFC}$  is the voltage, and  $V_{MFC}$  is the cell volume.

## 2.5 Analysis of bacterial community

The biofilm formed on the carbon cloth electrodes from the anodes was used for DNA extraction using a PowerSoil DNA Isolation Kit (Mo Bio Laboratories, Inc. Carlsbad, CA) according to the manufacturer's instruction. Total genomic DNA was used as template for PCR amplification of approximately 1500 pb of 16S rDNA with a forward primer (27f, 5'-AGAGTTTGATCCTGGCTCAG-3') and a reverse primer (1492r, 5'-GGTACCTTGTAAACGACTT-3') [20]. The PCR products were purified and cloned into TOPO TA cloning vector pCR2.1 according to the manufacturer's instructions (Invitrogen, Carlsbad, CA). Then they were transformed into competent cells of *E. coli* XL1-Blue by electroporation. White transformants were transferred to plates containing LB broth (25  $\mu$ g/mL kanamycin and 200  $\mu$ g/mL ampicillin), grown overnight at 37°C. Plasmids were isolated using High Pure Plasmid kit (ROCHE, Indianapolis, IN) subsequently clones were digested (2 h, 37°C) with *EcoRI* (BioLabs, New England) for the presence of inserts.

### 2.5.1. Sequencing and phylogenetic analysis

Inserts were sequenced on the sense and antisense stands at the Instituto de Biotecnología de la Universidad Nacional Autónoma de México using a Taq FS Dye Terminator cycle fluorescence-based sequencing with an automated capillary sequencer (Perkin Elmer, model 3130xl, Applied Biosystems). The sequencing reaction was performed using M13F-pUC (5'-GTTTCCCAGTCACGTTGTA-3') and M13R-pUC (5'-TTGTGAGCGGATAACAATTTC-3'). 16s RNA gene sequences of approximately 1500 nucleotides retrieved from each clone were assembled and edited using Bioedit. All sequences were further analyzed with Bellerephon chimera check program and with BLAST program (National Center for Biotechnology Information) [21] to determine the closest available database sequences. Multiple sequence alignments were performed using ClustalW and MEGA 5.0 software. Phylogenetic analyses were performed aligned sequences by the Neighbor-Joining algorithm with Kimura 2 parameter distance and bootstrapping of 1000 replicates in the Phylip program.

## 3. RESULTS AND DISCUSSION

### 3.1. Determination of internal resistance

The polarization curves and the power variation with current intensity of the MFC-P connected in series and parallel, and MFC-S are shown in Fig. 3A, Fig. 3B and Fig 3C, respectively. The internal resistances were calculated as the slopes of the sets of aligned points of the corresponding polarization curves; the values were 600 and 67  $\Omega$  for the MFC-P connected in series and parallel, respectively, and 4 600  $\Omega$  for MFC-S (Table 1). The values of the resistances for each face of the MFC-P were 330, 308, 306, 305, and 348  $\Omega$ .

The EIS data were represented in the form of Nyquist plots of the MFC-P connected in series and parallel, these data are shown in Fig. 4A and Fig. 4B. The internal resistances were calculated as the sum of  $R_1$ ,  $R_2$  y  $R_3$  of the equivalent circuits, the values were 602 and 57  $\Omega$  for the MFC-P connected in series and parallel, respectively.

The new design connected in series and parallel, lead to significant reductions of cell internal resistance, compared to the standard

cell (by 82 and 98%). This reduction in resistances values may be ascribed to the ‘sandwich’ assembly of the CMA. The significant decrease of  $R_{int}$  with decrease of inter-electrode distance is consistent with previous experiments on the effect of electrode spacing on internal resistance of MFC [8-9,12-13]. In particular, the proportion of  $R_{int}$  decrease in our work was similar to that reported elsewhere [5]; it was found a 70% reduction in  $R_{int}$  value in a single chamber MFC fitted with a ‘sandwich’ CMA, compared to a second cell where the electrodes were separated 7.8 cm. Furthermore in our work, parallel connection of multiple electrodes of MFC significantly increased  $P_{V-max}$  compared to  $P_V$  of both the MFC-P connected in series and MFC-S (Table 1).

Table 1 shows the maximum and average main response variables of the MFC-P and MFC-S in this work. All response variables were higher in the new design MFC-P than in the MFC-S, confirm the better performance of MFC-P. Maximum volumetric powers  $P_V$  in MFC-P connected in series and parallel were 62 and 569  $mW/m^3$ , respectively, and anode density powers  $P_{An}$  of the MFC-P connected in series and parallel were 3.2 and 29.6  $mW/m^2$ , respectively; these values were superior to those of the MFC-S (4.34  $mW/m^2$  and 52.07  $mW/m^3$ ). The improvement in  $P_V$  was probably due to the combined effects of increased  $\xi$  and decrease of  $R_{int}$ .

When the faces of the cell were connected in series, the voltage was 0.52 V ( $R_{ext}= 68$  k $\Omega$ ); this voltage was similar to that obtained when the faces if the MFC were connected in parallel (0.5 V). One approach to increase MFC voltages is to connected multiple MFC in series, forming a stacked system. However, when this is done the stack usually undergoes voltage reversal, resulting a low or nearly zero stack voltage. Voltage reversal has been shown to occur when anode potentials become unbalanced, for example when substrate concentration are low in one cell relative to an adjacent cell. The bacteria are less active at the lower substrate concentration; as a result, the anode potential of that cell becomes positive and similar to the cathode potential of the adjacent cell. Voltage reversal can also be driven under high curret even without substrate depletion. Voltage reversal occurring in only one of multiple MFCs connected in series results in a failure of the whole system [22-25].

The parallel connection substantially lowered internal resistance, this decrease could be attributed to the increased cross section area of the ion flow path due to parallel connection. Also, calculations using the Ohm’s law for parallel resistance connection closely

Table 1. Average values of several variables in cell characterization in this work.

Parameter	MFC-S <sup>a</sup>	MFC-P <sup>b</sup> Series	MFC-P <sup>b</sup> Parallel
$R_{int}$ ( $\Omega$ )	4600 $\pm$ 250	600 $\pm$ 32	67 $\pm$ 3
$P_{An-max}$ <sup>c</sup> ( $mW/m^2$ )	4.3	3.2	29.6
$P_{V-max}$ <sup>d</sup> ( $mW/m^3$ )	52.1	62.1	569
$E_{MFC-max}$ (V)	0.52	0.52	0.5
$I_{MFC-max}$ (mA)	0.1	1.1	7.5
$P_{MFC-max}$ (mW)	0.008	0.06	0.585

Notes: <sup>a</sup>Microbial fuel cell standard; <sup>b</sup>Microbial fuel cell parallelepiped (new design); <sup>c</sup>Maximum power density; <sup>d</sup>Maximum volumetric power.

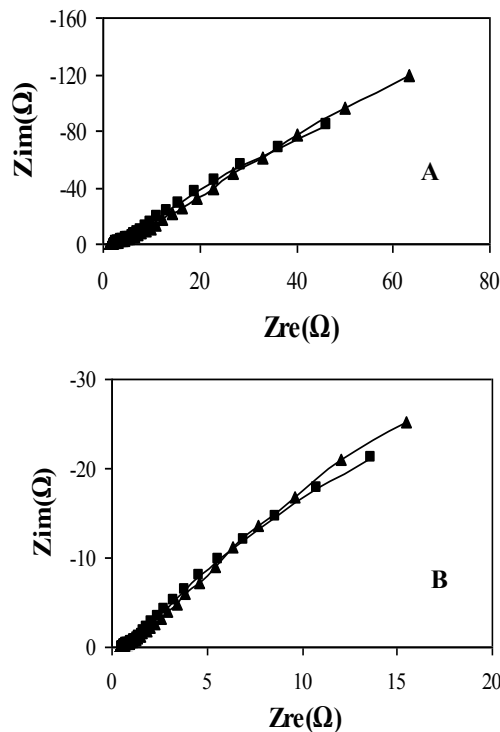


Figure 4. Nyquist plots of new design microbial fuel: (A) connection in series and (B) connection in Parallel

agrees with the total experimental value of  $67 \pm 3 \Omega$ . In effect,

$$1/R_{int\ total} = \sum (1/R_{int,j}), j = 1, \dots, 5 \quad (4)$$

When substituting the  $R_{int,j}$  of each face, Eq. 4 gives  $R_{int\ total} = 63 \pm 4 \Omega$ , this calculated value is very close to the experimental one obtained with the polarization curve method ( $67 \pm 3 \Omega$ ).

Parallel connection decreased not only the internal resistance by increasing the cross sectional area for ion flow, but also possibly by decreasing the electrode overpotential due to increase of the total electrode surface area, thereby leading to the production of maximum power at relatively high current output without significant energy losses [26]. Parallel connection of multiple electrodes of MFC significantly increased  $P_{V-max}$  compared to  $P_V$  of both the MFC-P connected in series and MFC-S (Table 1).

On the other hand, series connection showed an inverse trend to that in the parallel connection. Energy loss in the series connection is known to be caused by lateral ion cross-conduction between electrodes. This phenomenon is common when fuel cell arrays sharing the same electrolyte are connected in series to increase voltage output [26].

The relatively low values of  $P_{An}$  obtained in this work could be due to absence of acclimation of the inoculum to the new substrate. Indeed, the inoculum used in our experiments was acclimated to a synthetic wastewater that contained sucrose and acetic acid, as well as sodium sulfate as electron acceptor. When the inoculum was transferred from the seed bioreactor to the cell, the substrate fed was a model extract that did not contain sucrose and sulphate. Moreover, the substrate was concocted with acetic, propionic and

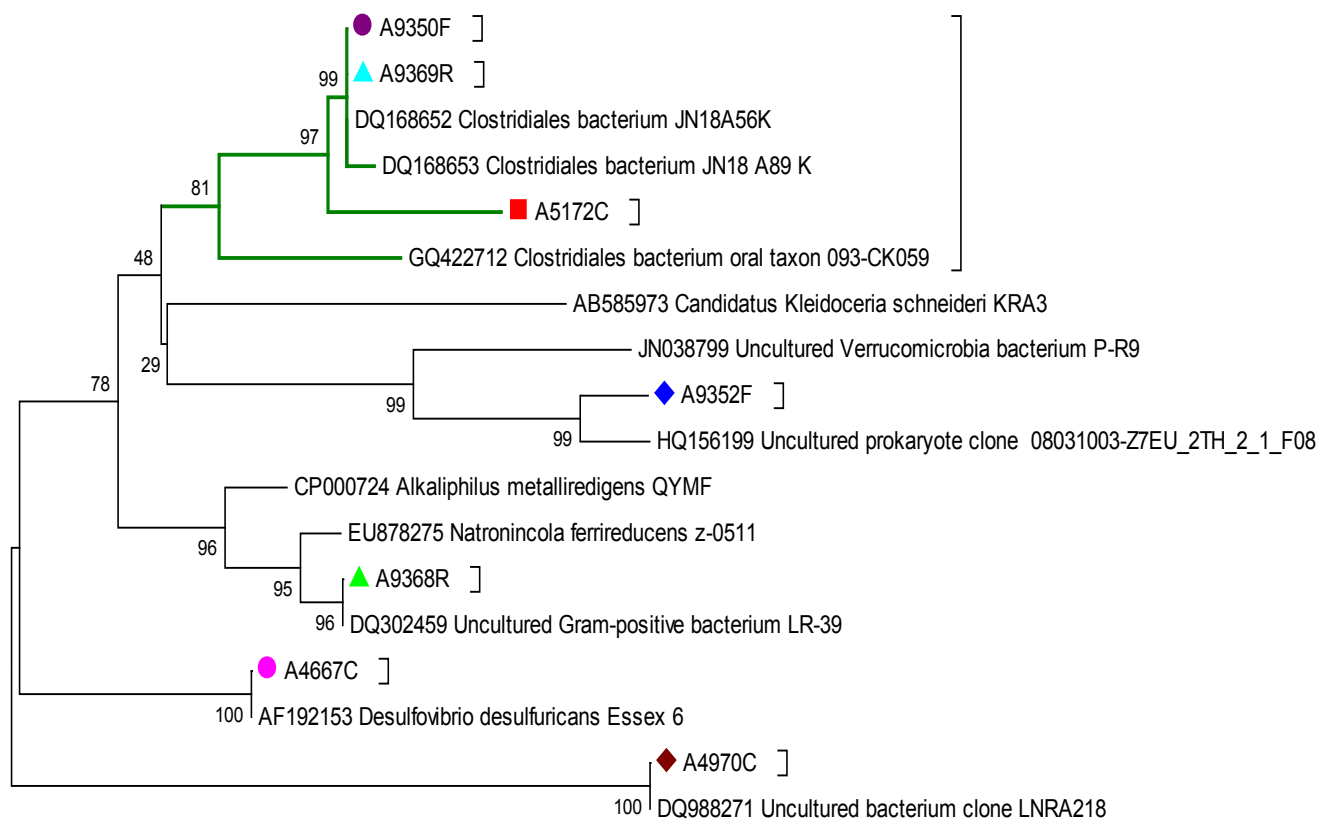


Figure 5. Phylogenetic relationships, based on 16S rRNA gene sequences. The cladogram was created using the neighbor-joining method of the MEGA application. The bootstrap consensus tree inferred from 1,000 replicates was constructed to represent the evolutionary distances of the taxa analyzed. The sequences analyzed are marked with colored symbol.

butyric acids as well as acetone and ethanol and mineral salts. So, the lack of acclimation to the new substrate probably had a negative effect on cell performance. Indeed, the inoculum was not previously subjected to selective pressures that could lead to its enrichment in electrochemically-active bacteria (EAB, also known as anodophilic or exoelectrogenic bacteria) [4]. As it is widely recognized, most of the EAB also are dissimilatory metal reducing microbes; their presence and dominance in the microflora anchored in MFCs are usually linked to significant power outputs [4].

Another factor involved in low average power could be the surface area of electrode materials. The positive effect of the larger anode surface area on power was demonstrated when several materials, such as plain graphite, carbon cloth, graphite foam were by adding graphite granules or using graphite fiber brushes in the MFC. Those materials are known to increase the electrode surface

area [27,28]. In our MFC-P, although we increase the electrode surface with the multiface approach, the total area is still lower than the available area reported for graphite granules and brushes. Moreover, the relatively large net or void volume of the anodic chamber could play a negative role on the intensive values of P (for instance  $P_V$ , etc.). Indeed, the geometric volume of the anodic chamber was 1 L whereas the volume occupied by the electrodes was 0.023 L; this gives a large chamber void volume of 0.977 L.

### 3.2. Phylogenetic analyses

Out of 9 clones originating from the MFC inoculated with sulphate reducing bacteria, 7 clones were selected. Their nucleotide sequences were determined. Table 2 shows that *Clostridia spp.* dominated of the whole on the biofilm of the MFC-P. The phylogenetic tree (Fig. 5) derived from this sequences group in a separate branch clearly shows that three clones found in our consortia were

Table 2. The bacterial diversity on biofilm of MFC-P

Clones	Similar relatives (type)	Identity (%)	Phylum (class)
Strain 1	<i>Desulfovibrio desulfuricans</i> (1)	100	<i>Proteobacteria</i> ( $\delta$ - <i>Proteobacteria</i> )
Strain 2	<i>Clostridiales bacterium</i> (3)	99	<i>Clostridia</i>
Strain 5	<i>Alkaliphilus oremlandii</i> (1)	96	<i>Firmicutes</i>
Strain 6	<i>Uncultured bacterium</i> (2)	100	<i>Uncultured bacterium</i>

affiliated to the clostridiales.

The major clones amplified from biofilm of the MFC-P were: *Clostridia* (42%), 98% identity with *Clostridiales bacterium*;  $\delta$ -*Proteobacteria* (16%), 99% identity with *Desulfovibrio desulfuricans*; *Firmicutes* (16%), 96% identity with *Alkaliphilus oremlandii*, and an *Uncultured bacterium* (26%) 93% identity with *uncultured bacterium*.

Our results are similar to those observed by Fung, *et al.* (2006) [29], who enriched electrochemically active bacteria in a MFC using glucose and glutamate (copiotrophic conditions); the enriched population consisted of  $\gamma$ -*Proteobacteria* (36.5 %), followed by *Firmicutes* (27%) and  $\delta$ -*Proteobacteria* (15%). On the other hand, Phung *et al.* (2004) [30], showed that the bacterial composition in a MFC fed with river water included  $\beta$ -*Proteobacteria*,  $\delta$ -*Proteobacteria*, *Acidobacteria*, *Chloroflexi* and *Verrucomicrobia*. Finally, Logan and Regan [31] demonstrated that the bacterial communities that develop in MFC show great diversity, ranging from primarily  $\delta$ -*Proteobacteria*, the predominate in sediments MFCs to communities composed of  $\alpha$ -,  $\beta$ -,  $\gamma$ - or  $\delta$ -*Proteobacteria*, *Firmicutes* and uncharacterized clones in other types of MFCs.

The bacterial population in the anodic biofilm of our cell was not as rich as found from other types of inocula. For instance, diversity given by Shannon-Weaver index was 1.3 [32], and the species evenness given by Pielou's evenness index [33] was 0.66, these values mean that diversity of inoculum was low and the evenness was between low-to-moderate, respectively. In the biofilm of the MFC-P there were *Deltaproteobacteria* clones; they are believed to be responsible for the direct electron transfer to the anode [30]. In addition, natural redox compounds such as sulfur/sulfide, Fe(II)/Fe(III) and humic acid were mentioned as possible mediators facilitating electron transfer from the microbial fuel cell to the electrode [34-39]. In our case, there was some free sulfide in the cell liquor (9.7 mmol/L).

#### 4. CONCLUSION

A new design of MFC whose main features were the assemblages or 'sandwich' arrangement of the cathode-membrane-anode and the extended surface area of electrodes (higher  $\xi$ ) exhibited a performance significantly superior to that of a similar cell (standard cell) where the electrodes were separated. The characterization experiments showed that the new design lead to significant reduction of cell internal resistances compared to the standard cell. The improvement in  $P_V$  was ascribed to the combined effects of increased  $\xi$  and decrease of  $R_{int}$ .

When the 5 faces of the MFC-P were connected in series, the  $R_{int}$  was 600  $\Omega$  with a voltage of 0.52 V. Characterization of the cell with the 5 faces connected in parallel gave a  $R_{int}$  of 62  $\Omega$  with a voltage of 0.5 V. On the other hand, the standard MFC-S exhibited a  $R_{int}$  values of 4600  $\Omega$  with a voltage of 0.47 V. Thus, the  $R_{int}$  of the new design MFC-P was significantly lower than that of the standard cell; this result was ascribed to both the changes in cell architecture and decrease of the inter-electrode distance. The  $P_V$  of the new MFC-P achieved values of 62 and 569 mW/m<sup>3</sup> for series and parallel connection, respectively, whereas the power delivered by the standard cell was much lower (52 mW/m<sup>3</sup>).

Our results confirm the positive effect of  $\xi$  on  $P_V$ , show the advantages of the 'sandwich' assemblage of AMC over separated electrodes, and demonstrate the convenience of parallel connection

of faces in multi-face MFC-P in order to further abate the internal resistance of the new design cell.

On the other hand, we demonstrated the successful application of molecular ecological techniques to analyze bacterial diversity, direct 16S rDNA analysis showed low species richness and low-to-moderate evenness. Microbial community anchored in the MFC-P consisted primarily of *Clostridiales bacterium* and *Desulfovibrio desulfuricans*, the last one is a member of  $\delta$ -subdivision of *Proteobacteria*. These bacteria are recognized to be capable of exocellular electron transfer, and are collectively defined as a community of "exoelectrogens".

#### 5. ACKNOWLEDGEMENTS

The authors wish to thank the Editors and Referees of *JNMES*, as well as the Chair and Referees of the Publications Committee of the SMH, for their careful reading of our MS and their insightful comments. CINESTAV-IPN and ICYTDF, Mexico provided financial support to this research. Areli del C. Ortega-Martinez received a graduate scholarship from CONACYT, Mexico. The excellent technical help with molecular biology analysis of Ms Ana Lilia Tirado-Chamú (BSBiochemEng) from IBT-UNAM, and personnel of Environmental of Biotechnology and Renewable Energy R&D Group CINESTAV-IPN is appreciated. Dr. Gerardo Vazquez-Huerta from the Fuel Cell and Hydrogen Group assisted with the EIS determinations.

#### REFERENCES

- [1] B.E. Logan, B. Hamelers, R. Rozendal, U. Schröder, J. Keller, S. Freguia, P. Aelterman, W. Verstraete, K. Rabaey, *Environ. Sci. Technol.*, 40, 5181 (2006).
- [2] H.M. Poggi-Varaldo, A. Carmona-Martínez, A.L. Vázquez-Larios, O. Solorza-Feria, *J. New Mat. Electrochem. Systems*, 12, 49 (2009).
- [3] Z. Du, H. Li, T. Gu, *Biotechnol. Adv.*, 25, 464 (2007).
- [4] H.M. Poggi-Varaldo, A. L. Vazquez-Larios, O. Solorza-Feria. "Celdas de Combustible Microbianas". Ed. F.J. Rodriguez-Varela, O. Solorza-Feria, E. Hernandez-Pacheco, Canada, 2010, p. 123.
- [5] A.L. Vazquez-Larios, G. Vazquez Huerta, F. Esparza-Garcia, E. Rios-Leal, O. Solorza-Feria, H.M. Poggi-Varaldo, *J. New Mat. Electrochem. Systems*, 13, 219 (2010).
- [6] H. Rismani-Yazdi, S.M. Carver, A.D. Christy, O.H. Tuovinen, *J. Power Sources*, 180, 683 (2008).
- [7] R. O'Hayre, S.W. Cha, W. Colella, F.B. Prinz, "Fuel cells fundamentals", John Wiley & Sons. New York, USA, 2005 p. 409.
- [8] G.W. Castellan, "Physical Chemistry", Addison-Wesley Publ. Co., MA, USA, 1966 p.581.
- [9] Y.Z. Fan, H.Q. Hu, H. Liu, *J. Power Sources*, 171, 348 (2007).
- [10] J.K. Jang, T.H. Pham, I.S. Chang, K.H. Kang, H. Moon, K.S. Cho, B.H. Kim, *Process Biochem.*, 39, 1007 (2004).
- [11] J.R. Kim, S. Cheng, S.E. Oh, B.E. Logan, *Environ. Sci. Technol.*, 41, 1004 (2007).
- [12] T. Song, Y. Xu, Y. Ye, Y. Chen, S. Shen, *J. Chem. Technol. Biotechnol.*, 84, 356 (2008).
- [13] H. Liu, S.A. Cheng, B.E. Logan, *Environ. Sci. Technol.*, 39,

- 5488 (2005).
- [14]D.Q. Jian, B.K. Li, *Water Sci. Technol.*, 59(3), 557 (2009).
- [15]I. Valdez-Vazquez, E. Ríos-Leal, F. Esparza-García, F. Cecchi, H.M. Poggi-Varaldo, *Int. J. Hydrogen Energy*, 30, 1383 (2005).
- [16]H.M. Poggi-Varaldo, L. Valdés, F. Esparza-García, G. Fernández-Villagómez, *Water Sci. Technol.*, 35, 197 (1997).
- [17]R. Sparling, D. Risbey, H.M. Poggi-Varaldo, *Int. J. Hydrogen Energy*, 22, 563 (1997).
- [18]P. Clauwaert, K. Rabaey, P. Aelterman, L. De Schampelaire, T.H. Pham, P. Boeckx, N. Boon, W. Verstraete, *Environ. Sci. Technol.*, 41, 3354 (2007).
- [19]APHA, “Standard Methods for the Examination of Water and Wastewater”, 17<sup>th</sup> edn., American Public Association, Washington DC, USA, 1989.
- [20]W.G. Weisburg, S.M. Barns, D.A. Pelletier, D.J. Lane, *J. Bacteriol.*, 173, 697 (1991).
- [21]S.F. Altschul, W. Gish, W. Miller, E.W. Myers, D.J. Lipman, *J. Mol. Biol.*, 215, 403 (1990).
- [22]Y. Kim, M.C. Hatzell, A.J. Idutchinson, B.E. Logan, *Energy Environ. Sci.*, 4, 4662 (2011).
- [23]P. Aelterman, K. Rabaey, H.T. Pham, N. Boon, W. Verstraete, *Environ. Sci. Technol.*, 40, 3388 (2006).
- [24]S.E. Oh, B.E. Logan, *J. Power Sources*, 167, 11 (2007).
- [25]S.H. Shin, Y. Choi, S.H. Na, S. Jung, S. Kim, *Bull. Korean Chem. Soc.*, 27, 281 (2006).
- [26]B. Wang, J.I. Han, *Biotechnol. Lett.* 312, 387 (2009).
- [27]H. Liu, S. Cheng, L. Huang, B.E. Logan, *J. Power Sources*, 179, 274 (2008).
- [28]Q. Deng, X. Li, J. Zuo, A. Liang, B.E. Logan, *J. Power Sources*, (2009).
- [29]C.Y. Fung, J. Lee, I.S. Chang, B.H. Kim, *J. Microbiol. Biotechnol.*, 16, 1481 (2006).
- [30]N.T. Phung, J. Lee, K.H. Kang, I.S. Chang, G.M. Gadd, B.H. Kim, *Microbiol. Lett.* 233, 77 (2004).
- [31]B.E. Logan, J.M. Regan, *Trends in Microbiol.*, 14, 512 (2006).
- [32]C.E. Shannon, *Bell System Technical J.*, 27, 379 (1948).
- [33]C.P.H. Mulder, E. Bazeley-White, P.G. Dimitrakopoulos, A. H., M. Scherer-Lorenzen, B. Schmid, “Species evenness and productivity in experimental plant communities”, *Oikos*, 104, 50 (2004).
- [34]B.H. Kim, H.S. Park, H.J. Kim, G.T. Kim, I.S. Chang, J. Lee, N.T. Phung, *Appl. Microbiol. Biotechnol.*, 63, 672 (2003).
- [35]G.T. Kim, M.S. Hyun, I.S. Chang, H.J. Kim, H.S. Park, B.H. Kim, S.D. Kim, J.W.T. Wimpenny, A.J. Weightman, *J. Appl. Microbiol.* 99, 978 (2005).
- [36]D.R. Lovley, *Curr. Opin. Biotechnol.*, 19, 564 (2008).
- [37]D.R. Lovley, *Nature Reviews Microbiol.* 4, 497 (2006).
- [38]C.A. Pham, S.J. Jung, N.T. Phung, J. Lee, I.S. Chang, B.H. Kim, H. Yi, J. Chun, *Microbiol. Lett.*, 223, 119 (2003).
- [39]D.E. Holmes, D.R. Bond, R.A. O’Neil, C.E. Reimers, L.R. Tender, D.R. Lovley, *Microb. Ecol.*, 48, 178 (2004).